

Review

Not peer-reviewed version

Advances in Carbon Dots-integrated Optical Fiber Sensors

[Kandasamy Sasikumar](#) , Gyeongchan Lee , [Ramar Rajamanikandan](#) , [Heongkyu Ju](#) *

Posted Date: 20 January 2026

doi: 10.20944/preprints202601.1563.v1

Keywords: biomarker; carbon dots; fluorescence; metal ion; optical fiber; sensing



Preprints.org is a free multidisciplinary platform providing preprint service that is dedicated to making early versions of research outputs permanently available and citable. Preprints posted at Preprints.org appear in Web of Science, Crossref, Google Scholar, Scilit, Europe PMC.

Copyright: This open access article is published under a [Creative Commons CC BY 4.0 license](#), which permit the free download, distribution, and reuse, provided that the author and preprint are cited in any reuse.

Review

Advances in Carbon Dots-Integrated Optical Fiber Sensors

Kandasamy Sasikumar ^{1,2,†}, Gyeongchan Lee ^{2,3,†}, Ramar Rajamanikandan ^{1,2} and Heongkyu Ju ^{1,2,*}

¹ Department of Physics and Semiconductor Science, Gachon University, Seongnam-si, Gyeonggi-do 13120, Republic of Korea

² Gachon Bionano Research Institute, Gachon University, Seongnam-si, Gyeonggi-do 13120, Republic of Korea

³ Department of Semiconductor Engineering, Gachon University, Seongnam-si, Gyeonggi-do 13120, Republic of Korea

* Correspondence: batu@gachon.ac.kr

† These authors contributed equally to this work.

Abstract

Carbon dots (CDs) have enormous potential in optical sensing applications because of their remarkable physicochemical properties. Benefiting from high specific surface area, rich active sites, bright photoluminescence, high photostability, and biocompatibility, CDs have been widely used as functional layers in optical fiber sensors, resulting in notable improvements in sensitivity, response speed, and environmental stability. This review describes recent advances in CD-integrated optical fiber sensors, with a focus on CD synthesis techniques and their integration with optical fibers for the sensing of diverse analytes, such as heavy metal ions, biomarkers, and dyes. CD-integrated fiber sensors exhibit significantly enhanced detection performance in terms of sensitivity, selectivity, repeatability, response time, and recovery time, compared to their non-CD counterparts. Finally, current challenges and future perspectives are discussed. This review aims to provide valuable insights for the design and development of novel CD-integrated optical fiber platforms for sensing chemically and biologically relevant analytes.

Keywords: biomarker; carbon dots; fluorescence; metal ion; optical fiber; sensing

1. Introduction

Carbon dots (CDs) are a class of zero-dimensional (0D) luminescent carbon nanomaterials with typical sizes of ~1–10 nm. They consist of a carbon core surrounded by abundant surface functional groups, such as hydroxyl, carboxyl, aldehyde, and amino groups. Depending on the degree of carbonization and the choice of carbon precursors, the core structure can be graphitic (sp^2) or amorphous (mixed sp^2/sp^3 hybridization) [1,2]. Based on their core structure and surface chemistry, CDs are generally classified into four categories: graphene quantum dots (GQDs), carbon quantum dots (CQDs), carbon nanodots (CNDs), and carbon polymer dots (CPDs) [3]. GQDs are small fragments composed of single- or few-layer graphene sheets (sp^2 hybridized). They are typically anisotropic, with relatively much larger lateral dimensions than their thickness. CQDs are almost spherical nanoparticles with carbon atoms arranged in a graphitic crystalline core (mixture of sp^2 and sp^3 hybridization). Both GQDs and CQDs show fluorescence and quantum confinement effects. In contrast, CNDs are highly carbonized, quasi-spherical nanoparticles with sp^2 and sp^3 hybridized carbon atoms; they are more amorphous and do not exhibit the quantum confinement effect. CPDs have a hybrid structure, comprising a carbon core attached with many organic polymer chains [4,5,6]. Despite their structural diversity, CDs possess several advantageous physicochemical characteristics, such as strong photoluminescence, good water dispersibility, excellent biocompatibility, low toxicity, and great photostability (resistance to photobleaching/photoblinking) [7,8]. Importantly, these

properties can be tuned via heteroatom doping, surface passivation, and surface functionalization strategies [9,10,11]. As a result, CDs have been identified as potential competitors to semiconductor quantum dots (QDs) and organic dyes, attracting significant attention in optoelectronics, sensing, catalysis, bioimaging, and drug delivery applications [12,13,14,15,16].

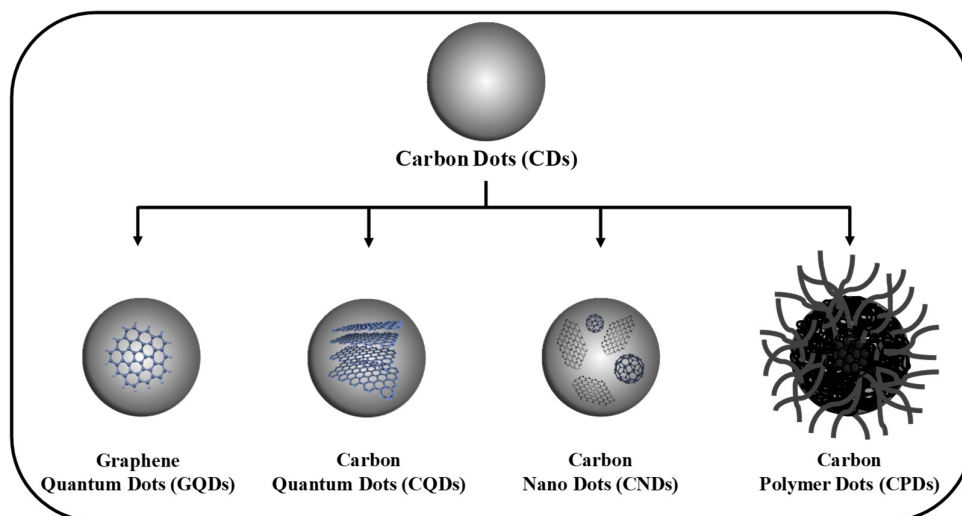


Figure 1. The classification of CDs: graphene quantum dots (GQDs), carbon quantum dots (CQDs), carbon nanodots (CNDs), and carbon polymer dots (CPDs).

In sensing technology, CDs have demonstrated excellent detection capabilities toward a wide range of chemically and biologically relevant analytes. Their sensing performance is governed by multiple mechanisms, such as Förster resonance energy transfer (FRET), inner filter effect (IFE), photoinduced electron transfer (PET), and dynamic or static fluorescence quenching [17,18,19,20]. Currently, several traditional analytical techniques, including high-performance liquid chromatography (HPLC), atomic absorption spectroscopy (AAS), atomic emission spectroscopy (AES), inductively coupled plasma-mass spectrometry (ICP-MS), gas chromatography with mass spectrometry (GC-MS), and electrochemical sensors, are used for the trace detection of analytes. These techniques are prominent for their sensing ability at very low concentrations, but they still struggle with limitations, including expensive instrumentation, complex operation, limited portability, and poor suitability for on-site analysis [21,22]. These drawbacks have motivated the development of simple, cost-effective, and rapid sensing technologies for in situ monitoring.

Optical detection methods are recognized as more advantageous due to their simple nature, high sensitivity, and quick response. Colorimetric sensors enable swift on-site sensing with the naked eye through visible color changes [23]. Fluorescence-based turn-off and turn-on sensors are good alternatives because of their high sensitivity, good selectivity, operational simplicity, and on-site usability [24,25]. In particular, optical fiber-based sensing platforms have emerged as powerful candidates for portable and remote sensing applications. Optical fiber sensors (OFSs) offer inherent advantages, such as strong resistance to electromagnetic interference, high sensitivity, corrosion resistance, structural flexibility, remote sensing capability, and compatibility with miniaturized systems. These features have enabled their extensive application in the field of environmental monitoring and the detection of chemical gases, biomarkers, and metal ions [26,27,28]. Many OFS interrogation techniques have been explored, including optical absorption, fluorescence-based sensing, fiber modal interference, fiber grating, and surface plasmon resonance (SPR) [29,30]. The integration of nanomaterials as functional transducer layers has further improved OFS performance [31,32]. In this context, CDs are particularly attractive owing to their tunable optical properties and versatile surface chemistry. In 2010, Gonçalves et al. earlier reported a CD-integrated OFS using sol-gel immobilized fluorescent CDs for Hg^{2+} detection in water [33]. Since then,

extensive research has been devoted to the development of CD-integrated OFS platforms for various sensing applications [34,35,36].

As of now, several reviews have addressed nanomaterial-based optical fiber biosensors and optical fiber sensing of specific analytes, as well as optical sensing applications of CQDs [29,37,38]. However, a comprehensive and focused review of CD-integrated OFS remains lacking. Motivated by this gap, the present review systematically summarizes recent progress in CD-integrated OFS platforms for the detection of chemically and biologically relevant analytes. We first outline common synthesis strategies for CDs, followed by a detailed discussion of CD-based OFS configurations and sensing mechanisms for metal ions, biomarkers, and other analytes. This review aims to provide a comprehensive reference and design guideline for advancing next-generation optical fiber sensing technologies based on CDs.

2. Synthesis Strategies of CDs

Current methods for the preparation of CDs are broadly classified into two categories: Bottom-up and Top-down methods (Figure 2). In the bottom-up approach, CDs are fabricated from appropriate carbon precursors through controlled carbonization. On the other hand, in the top-down approach, bulk carbon materials are broken into quantum-sized (< 10 nm) CDs via physical, chemical, or electrochemical processes.

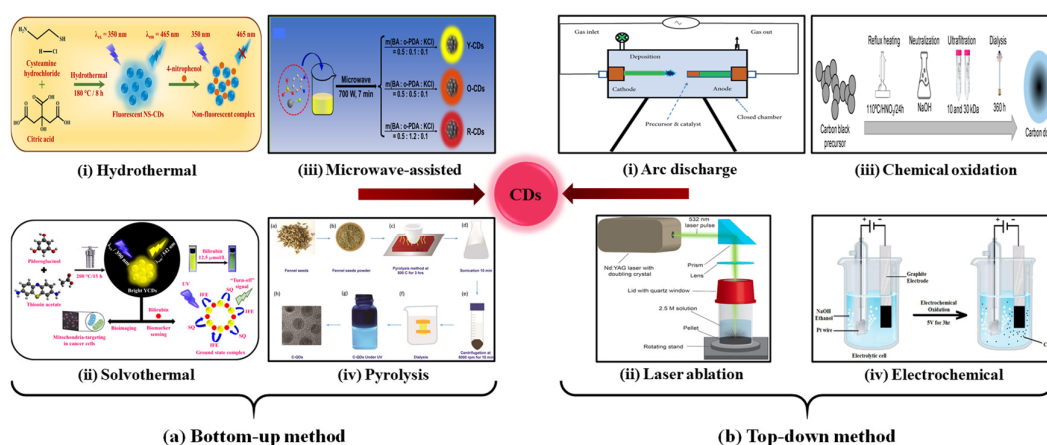


Figure 2. Synthesis methods of CDs. (a) Bottom-up method: (i) hydrothermal. Reproduced with permission from Ref. [39]. Copyright 2024, Springer. (ii) solvothermal. Reproduced with permission from Ref. [40]. Copyright 2024, American Chemical Society. (iii) microwave-assisted. Reproduced with permission from Ref. [41]. Copyright 2023, American Chemical Society. (iv) pyrolysis. Reproduced with permission from Ref. [42]. Copyright 2019, Springer Nature. (b) Top-down method: (i) arc discharge. Reproduced with permission from Ref. [43]. Copyright 2022, Sage Publications. (ii) laser ablation. Reproduced with permission from Ref. [44]. Copyright 2019, American Chemical Society. (iii) chemical oxidation. Reproduced with permission from Ref. [45]. Copyright 2022, MDPI. (iv) electrochemical. Reproduced with permission from Ref. [46]. Copyright 2022, Frontiers.

2.1. Bottom-Up Method

The bottom-up method provides significant advantages over the top-down method, including reduced processing time, environmental compatibility, and easy control over the chemical composition of CDs. During or after the synthesis process, functional groups can be easily attached to the CDs' surface, which offers extra advantages for binding with organic/inorganic target molecules in sensing applications. Owing to these benefits, bottom-up methods are extensively reported in the literature. In a typical bottom-up approach, organic precursors are dissolved in an appropriate solvent and subjected to thermal treatment for a particular time, leading to dehydration, followed by carbonization. Among the different bottom-up methods, hydrothermal/solvothermal, pyrolysis, and microwave-assisted synthesis are frequently used.

2.1.1. Hydrothermal/Solvothermal

The Hydrothermal/solvothermal route has developed as a prominent strategy because of its relatively facile and inexpensive synthesis. In this method, precursor materials are dissolved in an aqueous/non-aqueous solvent, sealed within a reaction vessel (Teflon-lined steel autoclave), and subjected to heat treatment at controlled temperature and pressure for a specific time to produce nanoscale CDs. The resulting CDs normally retain rich functional groups. Their PL characteristics can be controlled by adjusting parameters, such as reaction time, reaction temperature, pH of the solution, precursor composition, and precursor ratio [47,48]. For example, the graphitization degree can be increased via extending the reaction time [49]. Such a structural modification in the carbon core may contribute to extended PL wavelength, higher photostability, and superior quantum yield (QY), which positively influences the sensing performance of OFS. Yang's research group demonstrated red fluorescent CDs using o-PD (o-phenylenediamine) and concentrated HNO₃ (nitric acid) as an oxidizing agent. The fluorescence properties of CDs were regulated by varying the amount of HNO₃ [50]. In our laboratory, cyan blue emissive NS-CDs were prepared from the mixture of citric acid (0.1 M) and cysteamine hydrochloride (0.2 M) in aqueous medium processed at 180 °C for 8 h [39]. Diverse precursors, such as waste biomass materials, can also be used for CD synthesis. In contrast to hydrothermal, the solvothermal method needs one or more non-aqueous solvents for CD synthesis.

2.1.2. Microwave Method

In this strategy, carbon precursors dissolved in polar solvents undergo uniform heating under microwave irradiation (wavelength range: 1 mm–1 m) [51]. Owing to the strong interaction between microwaves and the carbon source, rapid and localized heating is achieved, allowing the production of CDs within a short time. The particle aggregation can be effectively suppressed by increasing nucleation sites, resulting in CDs with a homogeneous size distribution. In addition, it is feasible to incorporate structural defects and oxygen functionalities in CDs. These features increase the electron transfer ability of CDs, thereby enhancing their sensitivity toward electron-deficient analytes [52]. Given its operational simplicity, eco-friendliness, and energy efficiency, the microwave route has become an effective strategy for CD fabrication.

2.1.3. Pyrolysis

Pyrolysis is a simple chemical technique for preparing CDs from organic precursors via high-temperature thermal treatment. This technique is solvent-free, but it needs strong acid or alkali agents to initiate the decomposition of the carbon precursors, which creates environmental concerns. The long process time and the separation of CDs from the solution are challenging. CDs produced from pyrolysis usually exhibit high QY. Inoue et al. fabricated CDs from fenugreek seeds at different pyrolysis temperatures. The crystallinity of the carbon core improved at elevated temperatures, which resulted in high QY (~30%) [53].

2.2. Top-Down Method

The top-down technique involves the fragmentation of bulk carbon materials into nanoscale domains. The breakup of rigid, distinct carbon structures (graphite and CNTs) typically leads to the creation of GQDs, while indistinct or amorphous carbon precursors (carbon soot and activated carbon) result in CQDs or CNDs. This approach requires expensive carbon precursors, high temperature, toxic organic solvents, long reaction times, and sophisticated instrumentation. Some renowned techniques include arc discharge, laser ablation, electrochemical, and chemical oxidation.

2.2.1. Arc Discharge

This technique involves producing a high-temperature plasma by applying a high voltage between two electrodes (cathode and anode), causing the graphite anode to vaporize and fragment into carbon nanoparticles. A portion of carbon atoms within these carbon nanoparticles undergoes

structural rearrangement and bond formation, giving rise to the creation of CDs [54]. Although CDs with favorable fluorescence properties can be produced through this technique, there are many challenges, such as nonuniform particle size, low QY, and impurities [55].

2.2.2. Laser Ablation

This method is based on the irradiation of carbon materials using a high-energy pulsed laser source [56]. Consequently, CDs are produced from vaporized carbon material under high-temperature and pressure conditions. The CD size can be optimized by controlling the laser irradiation time, pulse repetition rate, pulse duration, laser wavelength, and laser power [57]. This approach allows surface functionalization, resulting in CDs with enhanced fluorescence characteristics. Using laser ablation, N-doped GQDs (QY ~9.1%) were derived from graphite flakes by Kim's research group [58]. The uneven particle size, limited control over morphology, and complex instrumentation are the drawbacks.

2.2.3. Chemical Oxidation

Chemical oxidation is a widely employed strategy that utilizes strong oxidizing agents to develop nanoscale CDs from large carbon materials. Different carbon precursors, including activated carbon, carbon black, carbon soot, resin, and starch, have been effectively converted into CDs [59]. Owing to the introduction of rich oxygen-containing functional groups during oxidation, aqueous dispersibility of the resulting CDs is significantly enhanced. Recently, bulk carbon materials (carbon black, activated charcoal, or graphite powder) were treated with HNO₃ and H₂SO₄ (1:1 volume ratio) by Yan's group to produce CDs with enzymatic catalytic activity exceeding 10,000 U/mg [60]. In Peng's work, the emission wavelength of CDs derived from carbohydrates was found to be strongly dependent on the chemical precursor and the duration of the HNO₃ treatment [61]. No sophisticated instrument is required, enabling efficient and scalable mass production of CDs. Nevertheless, the use of strong oxidizing agents raises concerns about environmental pollution.

2.2.4. Electrochemical

A conductive carbon source (graphite rod) is used as the working electrode in the electrochemical approach. Other carbon materials such as graphene films, carbon nanotubes (CNTs), coal-based carbon rods, and carbon fibers have also been utilized [59]. Due to its operational simplicity, high yield, and capacity to create uniform particle size, this method has become a popular choice. Particularly, the CDs' structural properties can be tuned by adjusting the electrolyte pH and concentration, applied potential, and reaction temperature [62]. Ming's group proposed the synthesis of pure CDs via a one-step electrochemical process using ultrapure water as an electrolyte [63].

3. Applications of Carbon Dots in Optical Fiber Sensors

3.1. Carbon Dots for Metal Ion Sensing

Metals, such as zinc, copper, and iron, are crucial for various enzymatic activities and biological processes in the human body [64]. But some metals, having a density (5 g/cm³) greater than water, are recognized as heavy metals, cause serious threats to human health and the environment. The prevalent heavy metals include arsenic, silver, cadmium, chromium, mercury, and lead, but also extend to aluminum, cobalt, manganese, molybdenum, titanium, nickel, and tin. Because of their bio-accumulative and non-biodegradable nature, they can cause acute toxicity even at low levels of exposure [65]. Thus, it is important to develop efficient optical sensors for the trace detection of heavy metals.

Iron (Fe) plays a crucial role in various biological processes, such as the storage and transport of oxygen to all body tissues, i.e., Fe²⁺/Fe³⁺ redox change in blood and other enzymatic reactions. But abnormal levels of Fe can lead to disorders like anemia, ischemia, and neurodegenerative diseases [66]. Therefore, CD-integrated OFS have been developed for the detection of Fe³⁺ ions [67]. Bian et al.

prepared N-CDs via a hydrothermal route using citric acid (carbon source) and urea (nitrogen source) at 200°C for 8 h [68]. The QY of N-CDs was 34.98%, and the zeta potential was found to be -18.4 ± 0.3 mV, making the N-CDs stable in water. Under 405 nm laser excitation, N-CD electrons are excited to higher energy states and release photons by radiative recombination upon returning to the ground state. When Fe^{3+} ions are introduced, the fluorescence emission is quenched due to the formation of the N-CDs/ Fe^{3+} complex, facilitated by the strong affinity between the half-filled 3d orbital of Fe^{3+} and the surface groups ($-\text{OH}$ and $-\text{COOH}$) of N-CDs. The fluorescence of NCDs could be restored by adding PO_4^{3-} . This was attributed to the formation of $\text{Fe}^{3+}/\text{PO}_4^{3-}$ complex by releasing N-CDs, as Fe^{3+} exhibited a stronger affinity for PO_4^{3-} than N-CDs. Various concentrations of polyethylene glycol diacrylate (PEGDA) were used to fabricate the core and cladding of the hydrogel optical fiber. First, solution A was prepared by mixing 2-hydroxy-2-methylpropiophenone (1% w/v) and PEGDA (80% w/v) with N-CDs in water. Next, without N-CDs doping, solution B was prepared by dissolving 2-hydroxy-2-methylpropiophenone (1% w/v) and PEGDA (40% w/v) in water. The injection of the solution A into a silicone hose, followed by the insertion of a plastic optical fiber, and 365 nm UV-induced photo-cross-linking, ultimately produced a fiber core. The fiber core was immersed in solution B and cured under a UV lamp to produce cladding. The laser beam (405 nm) reached the hydrogel optical fiber along the plastic fiber and excited the fluorescence. The hydrogel optical fiber was immersed in Fe^{3+} solution, and the backscattered fluorescence signal was detected by the spectrometer. The hydrogel OFS showed good sensitivity for 8% concentration of N-CDs at 24 °C, and 90 s response time. The sensor also demonstrated good linearity in the Fe^{3+} sensing in the range of 0–60 $\mu\text{M/L}$ with a LOD of 0.802 μM . Due to its excellent biocompatibility and nontoxicity, the proposed sensor can find an avenue in the biomedical field.

An optical fiber sensing platform was constructed by Cai's group, consisting of a laser source (375 nm), a sensing unit (with a 50:50 fiber coupler), and a detector [69]. The sensing unit was comprised of a spherical tip (200 μm diameter), which was prepared at the end of a multimode fiber (core/cladding diameter: 105/125 μm) using a fusion splicer and inserted into the hydrogel solution. The fiber end was connected to a UV light source. CQDs were synthesized from DL-malic acid and ethanolamine. They were dissolved in the hydrogel precursor solution, which consisted of PEGDA (700 Da, 38% (w/v)) and 2-hydroxy-2-methyl-propiophenone (photoinitiator, 1.8% (w/v)). This hydrogel was polymerized on the spherical tip surface by UV irradiation. From the optical simulation results, the spherical optical fiber tip was superior to the flat fiber tip, as the design of the spherical tip limited lateral overgrowth of the hydrogel. The PEGDA hydrogel film was in situ polymerized under UV irradiation on the fiber tip. The size and shape of the sensitive film rely on the UV light route through the fiber tip. The hydrogel film was in situ polymerized on the fiber tip under UV light (irradiation time: 0, 2, 7, 12, and 15 s). The fluorescence intensity increased with the size of the sensing probe. The probe with optimized UV irradiation time (12 s) was adopted in the optical sensing platform. Owing to the photoinduced electron transfer process, the fluorescence was enhanced upon the addition of Fe^{3+} ions. Using this sensing platform, Fe^{3+} ions could be quantitatively detected over a concentration range of 0–250 μM in 6 s, achieving a remarkable LOD of 0.6 μM . In another study, Cai et al. [70] fabricated a CQDs-based ratiometric fluorescence sensor for Fe^{3+} sensing, achieving a LOD of 0.4 μM in the range of 0–40 μM . Despite their outstanding sensing performance toward target metal ions, sensors using hydrogel may face challenges in terms of durability and stability during the detection process.

Very recently, Crawford's research group synthesized CDs using an acid–base reaction [71]. CDs were prepared by reacting ethanolamine and phosphoric acid in the presence of m-PD (carbon source). The chemical reaction was driven by the heat (110 °C temperature) generated; the choice of acid and base also influenced CD functionalization. However, the QY ($9.6 \pm 0.8\%$) was lower than values reported for the solvothermally prepared m-PD-based CDs. For sensing Fe^{3+} ions in acid mine drainage (AMD) sites, the unpurified CDs were combined with a portable fiber optic spectrometer (FOS) platform that utilizes a bifurcated optical fiber with a light-emitting diode (LED, 365 nm) excitation source. The characteristic green emission (510 nm) of CDs was quenched with increasing concentrations of Fe^{3+} ions (Figure 3a), exhibiting a linear Stern-Volmer profile for up to ~600 ppm Fe^{3+} (Figure 3b). The portable sensor achieved

a longer linear dynamic range, attributed to the weaker excitation source, excitation/emission collection paths, and the use of less pure CDs. The plot of emission peak area over time indicates that the emission suddenly responded upon the addition of Fe³⁺ (Figure 3c). The sensor showed a LOD of 2.2 ± 0.3 ppm. From the UV-Vis analysis, the increase in absorbance upon the addition of Fe³⁺ to the CD solution is consistent with the formation of the CD-Fe³⁺ complex. Also, luminescence lifetime slightly decreased for the CD-Fe³⁺ complex, signifying a static quenching mechanism. The dynamic quenching process also contributed to emission quenching, but only at higher Fe³⁺ concentrations (> 100 ppm), implying static quenching was the main quenching mechanism. Moreover, there was a partial overlap between the Fe³⁺ absorption spectrum and the CDs excitation spectrum, indicating that the inner filter effect also played in the quenching mechanism.

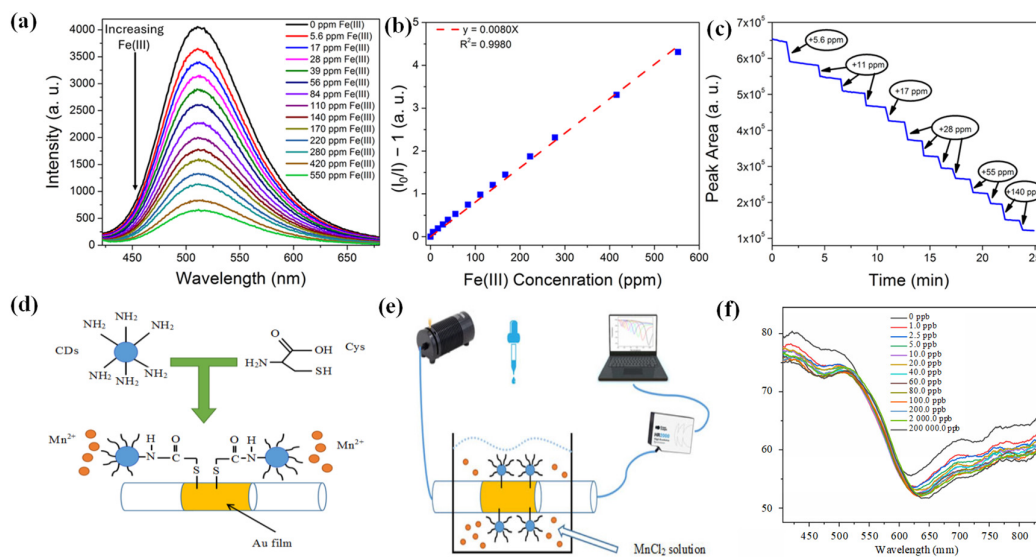


Figure 3. (a) Emission spectra of CDs in water exposed to increasing concentrations of Fe³⁺. (b) The corresponding Stern–Volmer plot. (c) Plot of emission peak area as a function of time, showing emission intensity drop for Fe³⁺ addition. Reproduced with permission from Ref. [71]. Copyright 2025, MDPI. (d) Immobilization of CDs on the Au film surface. (e) Sensor setup for Mn²⁺ detection. (f) Variation of the SPR curve with different concentrations of Mn²⁺ solution. Reproduced with permission from Ref. [72]. Copyright 2025, Springer Nature.

Fu et al. proposed an OFS for Mn²⁺ detection, combining the advantages of CDs and the SPR sensor. As depicted in Figure 3d, two fibers (single-mode and multimode fibers) were fused to form an SPR-sensitive part [72]. Their inner core diameters were 3.8 and 110 μm, respectively, while the outer cladding size was 125 μm. The CDs were immobilized on the Au film using cysteine. The –SH group on cysteine formed Au–S with Au NPs, and the –COOH connected CDs to AuNPs. The sensor setup is illustrated in Figure 3e. The sensing region was immersed in the analyte solution, and the fiber ends were linked to the spectrometer and light source. The negative zeta potential of CDs promoted strong electrostatic attraction toward Mn²⁺ ions. Moreover, the high selectivity of CDs was due to the strong affinity of Mn²⁺ ions with the amino groups (electron-donating) of CDs. Due to the introduction of CDs, the performance was exponentially increased. The SPR curve varies with different concentrations of Mn²⁺ solution, which is displayed in Figure 3f. As a result, it exhibited a good sensitivity of 6.383 nm/lg(ppb) (0–200 ppb) on Mn²⁺ ions, with the detection limit of 0.3462 ppb. The sensor was practically applied for sensing Mn²⁺ in blood serum and natural water resources.

Zhou et al. developed a highly sensitive SPR-based sensor for Fe³⁺ detection using a structurally simple, multimode-coreless-multimode optical fiber [73]. The fiber was coated with an Au film (~60 nm thickness) modified by Au nanoparticles (AuNPs), whose refractive index (RI) sensitivity was 3440.45 nm/RIU. On top of this layer, functionalized CQDs were immobilized. The CQDs were hydrothermally synthesized using sodium lignosulfonate and p-PD (200 °C for 9 h). The –COOH and –OH groups

facilitated CQDs to form a complex Fe^{3+} , effectively immobilizing Fe^{3+} on the fiber surface, realizing specific Fe^{3+} detection. The as-designed sensor demonstrated an excellent sensitivity of 2.07 nm/lg (M) in the concentration range of 10^{-12} – 10^{-2} M with a detection limit of 2.88×10^{-13} M. Thus, for Fe^{3+} detection, SPR-based sensors exhibit higher sensitivity with the lowest LODs compared to conventional sensors. However, the proposed sensor has the drawback of a long sensing time of 30 min.

In another work, N, S codoped CDs were employed in an interferometric optical microfiber sensor [74]. The sensing system was composed of a broadband superluminescent light-emitting diode (1525–1570 nm), optical microfiber sensor, and an optical spectrum analyzer (Figure 4a). Citric acid and thiourea were used to synthesize N, S-CDs (size $\sim 3.27 \pm 0.58$ nm) through the microwave method (800 W/6 min). Unlike traditional CD-based sensors that rely on fluorescence quenching in liquid media, this sensor operated in the solid phase, where CDs acted as a chelating agent on the tapered fiber surface. Figure 4b shows the effective refractive indices for fundamental mode (HE_{11}) and higher-order mode (HE_{12}) across diverse refractive indices at the cladding–medium interface of the tapered region and the corresponding phase difference between the two modes. The phase difference contributes to an output spectrum shift (Figure 4c). When Fe^{3+} binds to the surface functional groups of the CDs, it causes a local refractive index change at the fiber–solution interface. This alters the phase difference between guided optical modes, producing a wavelength shift in the interference spectrum. The sensor demonstrated a linear response in the range of 0–300 $\mu\text{g/L}$, with a sensitivity of 0.0061 nm/($\mu\text{g/L}$) and a LOD of 0.77 $\mu\text{g/L}$.

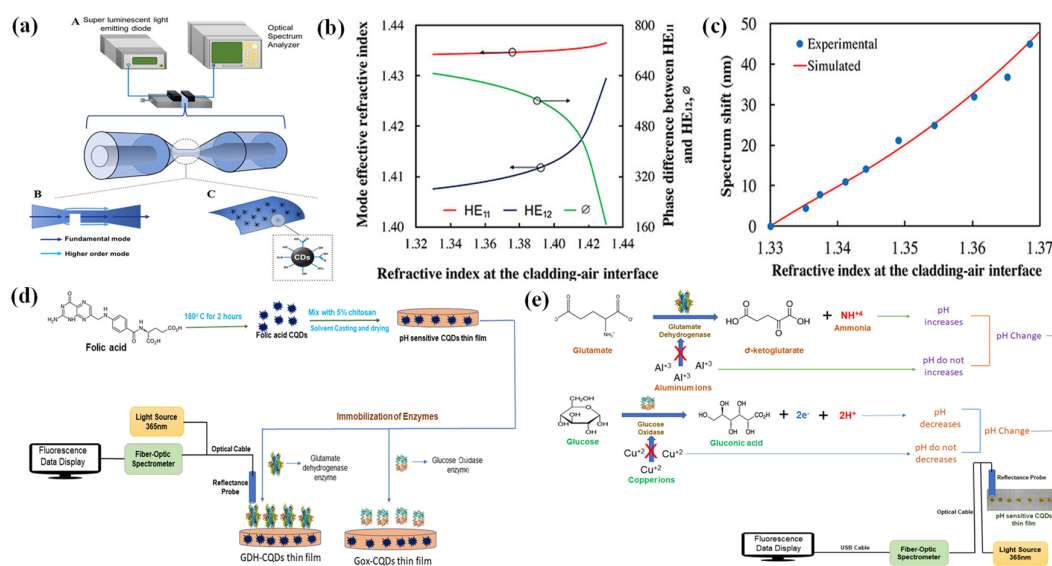


Figure 4. (a) Illustration of the sensor, sensing principle, and molecular structure of N, S-CQDs. (b) Simulated effective refractive index for HE_{11} and HE_{12} modes at diverse refractive indices of the cladding–medium interface and the phase difference between the two modes. (c) Spectrum shift as a function of the refractive index of the cladding–medium interface. Reproduced with permission from Ref. [74]. Copyright 2019, American Chemical Society. (d) GDH/Gox-CQDs chitosan film biosensor. (e) Sensing mechanism for the detection of Al^{3+} and Cu^{2+} ions. Reproduced with permission from Ref. [78]. Copyright 2023, American Chemical Society.

Lead (Pb) is one of the hazardous heavy metals to humans and animals. Chronic exposure to Pb^{2+} causes the development of cardiovascular, reproductive, and neurodegenerative (Alzheimer's and Parkinson's) diseases [75]. Thus, the development of efficient and reliable strategies for the trace level detection of Pb^{2+} is urgently required. Hence, Joshi et al. developed a fluorescent FOS-based chemosensor using folic acid-CQDs [76]. The portable, on-site sensor was relatively cheaper than the conventional microwave plasma-atomic emission spectroscopy (MP-AES). CQDs were synthesized from folic acid dissolved in water (heated at 180 °C for 2 h). Then, they were mixed with dithizone (10% w/v) with a solution of acetic acid (2% v/v) containing chitosan (5% w/v), and the solution was

stirred for 15–20 min and allowed to evaporate to finally produce the polymerized thin films. The CQD thin films exhibited good photostability (> 60 days) with only about 3–4% fluorescence intensity drop. The stability of the chitosan in the pH range of 4–8 and dithizone–Pb²⁺ complex formation enabled the Pb²⁺ sensing. Due to the formation of the dithizone–Pb²⁺ complex, CQD embedded in the chitosan thin films is exposed to the protons produced, resulting in the quenching of CQD's fluorescence. The pH variation can be recorded from the fluorescence intensity changes at 486 nm. The sensor was coupled to a reflectance probe connected to an FOS system. At 365 nm excitation, the fluorescence emission was observed at 486 nm using the FOS device. The estimated analytical parameters were compared with the results of MP-AES. Both methods showed linear regression coefficient (R²) greater than 0.99 in the detection range of 0–100 μM. The CQD-dithizone sensor achieved remarkable accuracy, with recoveries close to 100% (100.60–100.78%) that were comparable to MP-AES (100.85–101.22%). The developed sensor, with real-time and point-of-care capabilities, showed a better sensitivity of 0.0091 units/μM for Pb²⁺ ions with a LOD of 18.3 nM. Notably, the response time (1 min) was superior to that of the MP-AES technique (8 min).

Higher concentrations of Cu²⁺ pose the risks of gastrointestinal disturbance, kidney and liver failure, and neurodegenerative diseases [77]. Vyas and Joshi built an enzyme-functionalized CQDs thin film biosensor for detecting Cu²⁺ and Al³⁺ ions in tap water and river water samples [78]. Folic acid-CQDs were immobilized within a chitosan matrix to form photostable, biocompatible thin films. The conjugating enzymes, glutamate dehydrogenase (GDH) and glucose oxidase (Gox), were electrostatically adsorbed onto the film layer to attain selective inhibition-based detection of metal ions. The fluorescence of the thin film was measured by an FOS connected to a reflectance probe. The schematic of the GDH/Gox-CQDs chitosan thin film sensor is depicted in Figure 4d. As shown in Figure 4e, the GDH converts glutamate into α-ketoglutarate, producing ammonium ions, thereby increasing pH and fluorescence intensity. But in the presence of Al³⁺ ions, fluorescence decreases due to the suppression of GDH activity. On the other hand, Gox primarily oxidizes glucose to gluconic acid, producing protons and reducing pH. Due to the presence of Cu²⁺ ions, Gox is inhibited, reducing acid formation, stabilizing pH, and stabilizing or increasing the fluorescence. The linear response range was 0–100 μM, with excellent LODs of 24 ppb (Al³⁺) and 19 ppb (Cu²⁺). The accuracy was about 100–102%. Compared to MP-AES, this sensor provided rapid, portable, and cost-effective point-of-care monitoring. The same research group also used a CQD-PVA thin film sensor to detect Co²⁺, Pb²⁺, Ni²⁺, Mn³⁺, and Cr³⁺ ions with a LOD range of 0.006–0.019 ppm with a linear range of detection as 0–100 μM [79]. In spiked real water samples, the sensor showed good accuracy (100–103%). A non-emissive ground state complex formation of a CQD thin film with metal ions resulted in the quenching of fluorescence intensity. A CD-based portable FOS for the luminescent detection of Co²⁺ ions was reported [80]. The emission spectrum of CDs overlapped with the quencher's (Co²⁺) absorption band at ~510 nm, leading to an emission quenching with the increase of Co²⁺ concentration. The low-cost sensor provided comparable performance to a commercial spectrofluorometer, achieved LODs of 0.7 ppm (in water) and 3.5 ppm (in pH 1.68 buffer). Moreover, the sensor showed a remarkable selectivity for Co²⁺ among 13 common metal ions.

3.2. Carbon Dots for Biomarker Sensing

Leptospirosis is an infectious zoonotic disease caused by the pathogenic spirochete of the genus *Leptospira*. The disease is difficult to diagnose as its early symptoms are similar to those of other febrile illnesses, such as dengue, malaria, and meningitis [81]. Therefore, a sensitive and highly specific detection strategy is crucial for the timely and accurate treatment of leptospirosis. Keeping this in mind, Yaacob and coworkers developed a biosensor for *Leptospira* DNA detection using a tapered single-mode fiber (SMF) (core ~9 μm, cladding ~125 μm) deposited with CQDs [82]. The optical fiber was connected to a broadband light source and an optical spectrum analyzer through single-mode patch cords. Transmission signals were displayed via a LabView™ program. Before probe DNA attachment, the CQDs-functionalized tapered optical fiber was treated with NaOH to enrich –OH groups on CQDs, followed by silanization using (3-Aminopropyl)triethoxysilane

(APTES) to form a silane monolayer, and further treated with glutaraldehyde. The RMS roughness and surface area increase after coating of CQDs on the tapered region, which is significant for good sensing performance by creating more available active sites to facilitate enhanced DNA adsorption. Since the crystalline structure of CQDs affords more stability and a high surface area, more probe DNA can be immobilized. Variation in NaCl concentrations affected the refractive index (RI), resulting in proportional wavelength shifts ($\Delta\lambda$) with a sensitivity of 2235.4 nm/RIU ($R^2 > 0.99$)—a 20% improvement over non-CQD fibers. Upon probe DNA immobilization and cDNA hybridization, a notable red shift (1.695–2.624 nm) confirmed successful surface modification and target binding. Owing to the incorporation of CQDs, the sensor affinity toward *Leptospira* cDNA was successfully enhanced, reaching a dissociation constant (K_d) of 0.552 nM. The proposed biosensor outperformed non-CQDs biosensors, attaining good linearity ($R^2 = 0.986$), sensitivity of 1.8295 ± 0.6 nm/nM, and an LOD as low as 1.0 fM. Specificity and cross-reactivity studies revealed negligible interference from non-target DNA and high selectivity for *Leptospira* serovars Canicola and Copenhageni, with wavelength shifts increased by ~25% compared to non-CQDs sensors. To further increase the sensitivity of the biosensor, this research team introduced a post-deposition annealing treatment (70 °C for 10 min) to tune CQDs' grain size, morphology, and crystallinity [83]. As a result, CQDs were strongly attached to the tapered optical fiber. Consequently, the sensitivity of the sensor was greatly enhanced to 2.321 ± 0.048 nm/nM ($R^2 > 0.99$), about 21% higher than the previous work.

Acetylcholine (ACh) is one of the common neurotransmitters in both the central and peripheral nerve systems, plays a vital role in memory, learning, and attention. ACh is associated with the neurodegenerative disorders, progressive dementia, motor dysfunction, Schizophrenia, etc. To address this issue, a highly sensitive, rapid, selective biosensor was built using a quartz optical fiber (600 μ m diameter) containing Acetylcholinesterase/N-CQDs/cellulose acetate (AChE/N-CQDs/CA) film [84]. N-CQDs were fabricated by a facile hydrothermal route. o-PD and sodium ascorbate were mixed in deionized (DI) water and heated at 180 °C for 9 h. The excitation and emission wavelengths of N-CQDs were about 350 nm and 440 nm, respectively. The cytotoxicity of N-CQDs was evaluated on SH-SY5Y cells. The AChE/N-CQDs/CA complex was synthesized by cross-linking and coated on the end face of the fiber by the dip-coating technique. The optical fiber fluorescence platform was constructed with a diode laser source (473 nm, violet), where the laser was coupled into an optical fiber core using an attenuator, a dichroic mirror, and a microscope objective lens (10x). The laser beam was transmitted along the core to the other end of the fiber and excited the N-CQDs on the sensitive film to emit a fluorescence signal. This signal was transmitted back along the fiber, received, and processed by the spectrometer and the computer. The probe was immersed in a 1.5 mL glass vial containing the ACh solution, and the resulting fluorescence emission was recorded. In the presence of AChE, an increase in the AChCl concentration (1 nM–500 μ M) resulted in a concentration-dependent decrease in fluorescence intensity, ascribed to a pH decrease by acetic acid in hydrolysis. The sensor displayed a rapid fluorescence quenching (within 1 min) and stabilization (within 5 min). The modified Stern-Volmer plot revealed a LOD of 0.29 nM and the highest sensitivity in the range of 1–10 nM. The biosensor also demonstrated a high selectivity. Compared with the interferents at higher concentrations (1000 nM), AChCl (100 nM) produced a pronounced change in fluorescence intensity.

A biosensor was fabricated using silica-functionalized CDs [85]. CDs were prepared from curcumin and dimethylformamide by the microwave method, functionalized with silica, and immobilized with laccase enzyme. The biosensor was immobilized on the fiber using ethyl cellulose by a dip-coating technique. The biosensor exhibited excellent sensitivity for dopamine with the lowest LODs of 46.4 nM. The biosensor was assessed for multi-color imaging in human neuroblastoma cells (SH-SY5Y) and optical fibers. The laccase enzyme oxidizes dopamine into dopaquinone, and photoinduced electron transfer occurs between CDs (electron donor) and dopaquinone (electron acceptor), leading to fluorescence quenching. Adrenaline (i.e., epinephrine) is a neurotransmitter that belongs to the catecholamine group, used to treat various conditions such as hypertension, bronchial asthma, myocardial infection, and Parkinson's disease. The concentration level of adrenaline is closely associated with Huntington's disease, cardiovascular constriction,

elevation of blood pressure, etc. Considering these issues, an OFS was constructed by immobilizing CQDs/cellulose acetate composite thin film on the fiber tip using the dip-coating technique [86]. The fluorescence intensity of the CQDs was quenched by adrenaline via a static quenching effect, resulting in a LOD of 1.4 μM with a good linear response in the range of 5–45 μM ($R^2 = 0.99875$).

3.3. Carbon Dots for Other Targets

Metal-organic framework (MOF) encapsulated with cobalt-doped CDs (Co-CD/PMOF) was developed for the detection of Aflatoxin-B1 (AF-B1) [87]. Figure 5a illustrates the hydrothermal synthesis of Co-CD/PMOF. Briefly, PMOF (porphyrin-based MOF) was first prepared, followed by the in situ doping of Co-CDs into the PMOF pore channels using CoCl_2 , citric acid, and ethylenediamine as precursors. The resulting bifunctional nanozyme exhibited both peroxidase-mimic activity and fluorescence property. AF-B1 detection was based on a dual-mode (chemiluminescence (CL)/fluorescence (FL)) immunoassay strategy using anti-AFB1 antibody-modified Co-CD/PMOF as the signal amplification nanoprobe. Unlike conventional flash-type CL emission, in this work, the glow-type CL emission contributed by oxygen radicals facilitated a highly sensitive CL platform. The CL mode sensing of AFB1 was conducted based on indirect competitive immune affinity. The AFB1-OVA antigen-functionalized OFS was employed as a bioreaction interface and CL transducer. As the concentration of AFB1 increased, the Ab-Co-CD/PMOF bound to the functionalized OFS reduced because more binding sites of Ab-Co-CD/PMOF were occupied by AFB1. Under the catalysis of Ab-Co-CD/PMOF, CL signals inverse to AFB1 concentrations were generated and then detected by OFS. The FL mode assay was achieved by a sandwich immunoassay. AFB1 targets were captured by AFB1 antibody-functionalized magnetic beads. Ab-Co-CD/PMOF could also bind with AFB1 targets through immunoaffinity. The as-formed Ab-Co-CD/PMOF/AFB1/functionalized magnetic beads structure increased with the AFB1 concentration, contributing to the increase of FL signal (Figure 5b). In the CL mode, the optical fiber sensing platform achieved a LOD of 0.217 ng/mL (detection range: 0.63–69.36 ng/mL). The FL mode was also highly sensitive, offering a LOD of 0.027 ng/mL (detection range: 0.54–51.91 ng/mL). As depicted in Figure 5c,d, interfering biotoxins such as Zearalenone (ZEN), ricin, Ochratoxin-A (OTA), and their mixture produced negligible effects on AFB1 measurement for both CL and FL mode assay strategies, signifying their good selectivity and anti-interference ability.

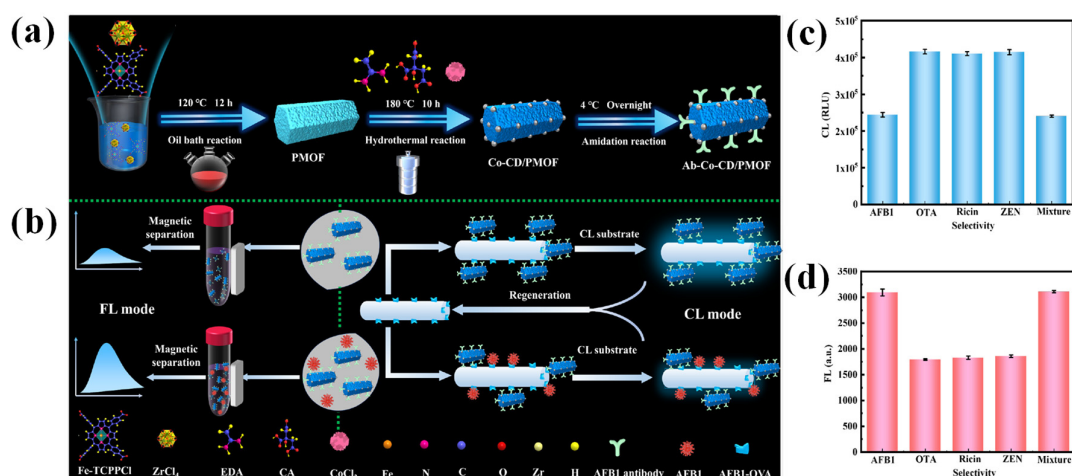


Figure 5. The detection of AFB1 using the CL/FL dual-mode strategy. (a) Synthesis of AFB1 antibody-functionalized Co-CD/PMOF nanoprobe. (b) The sensing mechanism of the Co-CD/PMOF dual-mode assay. Selectivity and anti-interference studies of the (c) CL mode assay, (d) FL mode assay (AFB1: 10 ng/mL, interferences: 100 ng/mL). Reproduced with permission from Ref. [87]. Copyright 2024, American Chemical Society.

SPR-based glucometer sensors have been reported by our group [88]. Using aniline-functionalized a-GQDs, a non-enzymatic fluorescence sensor was developed for glucose sensing [89]. With the combination of phenyl boric acid (PBA), the sensor exhibited “turn-off” (fluorescence quenching), and the a-GQDs/PBA system showed a “turn-on” mechanism for glucose sensing. This fluorescence recovery was due to the dissociation of the PBA linker from a-GQDs as the PBA's boronic acid groups formed negatively charged boronic ester complexes with the cis-diols of glucose. The a-GQDs/hydrogel film OFS demonstrated a LOD of 2.1 μM . Due to its high biocompatibility, the a-GQD/PBA system was used for glucose detection in HeLa cells. Taking advantage of the large mode area and high optical transmission efficiency of quartz fiber, a CQDs-GOD/CA biosensor was also developed [90]. The enzymatic CQDs-GOD complex was the fluorescence indicator.

Hydrazine is a reducing agent typically used in the manufacturing of polymers, insecticides, and pharmaceuticals. Due to its carcinogenic, mutagenic, and neurotoxic effects, as well as environmental contamination effects, sensitive and selective detection of hydrazine is urgently required to ensure human health and environmental safety. An optical fiber thin film chemosensor was designed for the real-time and specific sensing of hydrazine, a toxic industrial pollutant, in water samples [91]. The sensor utilizes a chitosan-based thin film co-immobilized with 2,4-dinitro-1-chlorobenzene (DNCB) and CQDs. The sensor demonstrated a quick response time (1 min) and a low LOD (7 ppb). The DNCB binds with hydrazine, producing a 2,4-nitrophenyl-hydrazine complex and HCl acid, thus resulting in the pH reduction. As the CQDs are highly pH-sensitive, the resulting H^+ ions quench the fluorescence of CQDs by accepting electrons. This process results in a quantifiable decrease in fluorescence emission intensity at 505 nm, allowing for the detection of hydrazine. Nitric oxide (NO) is a biological messenger that is widely involved in regulating neural signaling, blood vessel dilation, and immune responses. Unregulated levels of NO in the human body may result in neurodegenerative and inflammatory bowel diseases. A fluorescent probe comprised of CQDs with o-PD groups was prepared to selectively detect NO [92]. The o-PD groups on the surface of CQDs can react with NO to form a non-fluorescent ground state complex with an aryl triazole structure (static quenching), leading to fluorescence quenching. The CQDs-based OFS was able to detect NO with a LOD of 9.12 nM. The sensor could be used to detect NO in human serum. A fluorescent optical fiber CQD thin film sensor was employed to detect textile dyes, viz., methyl red, bromocresol green, methyl orange, and methylene blue, in a linear range of 0–100 μM , with the corresponding LODs of 26.4 ppb, 46.2 ppb, 214.5 ppb, and 29.7 ppb, respectively [93].

4. Conclusions and Future Perspectives

This review has summarized recent advances in carbon dots (CDs)-integrated optical fiber sensors (OFSs) for the detection of heavy metal ions, biomarkers, and other chemically and biologically relevant analytes. Owing to their compact size, immunity to electromagnetic interference, and structural flexibility, OFSs have emerged as powerful sensing platforms. Different optical interrogation techniques, including fiber grating, fiber modal interference, fluorescence, optical absorbance, and SPR, have been successfully combined with CDs to achieve sensitive analyte detection. Irrespective of these strategies, sensing performance is mainly governed by the intrinsic properties of CDs, which contribute to improved sensitivity, high selectivity, LOD, and rapid response. As multifunctional nanomaterials, CDs present high surface area, abundant functional groups, tunable photoluminescence, and excellent aqueous dispersibility, enabling them to be used either as standalone sensing layers or in hybrid configurations with other functional materials. When immobilized on optical fibers, CDs facilitate strong interactions with target analytes through complexation, electrostatic attraction, photoinduced electron transfer, inner filter effects, and refractive index modulation. As a result, CD-integrated OFSs have demonstrated LODs at the μM , nM, and even fM levels for analytes, highlighting their remarkable signal amplification ability.

Despite these promising advances, there are still several challenges in the development of related optical sensors. First, advanced fiber configurations, such as tapered, U-shaped, spherical tip, interferometric microfiber structures, have been successfully demonstrated to improve light-matter

interaction and sensing performance, but they may compromise mechanical robustness and long-term stability. Therefore, it is necessary to carefully optimize fiber structures as well as interrogation strategies. Second, optical fiber design processes (fiber fusion, cladding removal) often require specialized equipment and technical expertise. SPR-based fiber sensors offer label-free detection with excellent sensitivity. However, it also needs expensive noble metal (Au, Ag, and Pt) nanoparticles and homogeneous film deposition. Third, the reliability of CD-integrated OFSs critically depends on the quality of immobilized CDs/CDs composite film on the fiber surface. Common coating methods, such as hydrogel polymerization, dip-coating, and electrostatic self-assembly, frequently suffer from a lack of film uniformity, weak adhesion, and poor reusability. Thus, coating and immobilization strategies should be improved to achieve smooth, uniform, and mechanically robust films. Finally, the reliable detection of trace analytes in real samples remains challenging due to matrix interference and environmental fluctuations. For example, temperature-induced changes in the photoluminescence of CDs and refractive index can affect the sensitivity of OFS.

In the future, the development of next-generation CD-integrated OFSs will need the synergistic integration of mechanically robust optical fiber configurations, highly photostable CDs, optimized fiber structures, and advanced immobilization techniques. With continued advances in CD preparation, optical fiber design, and interrogation approaches, CD-integrated OFSs are anticipated to play a vital role in environmental monitoring and biosensing applications.

Author Contributions: **Kandasamy Sasikumar:** Conceptualization, Methodology, Data curation, Formal analysis, Investigation, Writing – original draft. **Gyeongchan Lee:** Conceptualization, Methodology, Data curation, Formal analysis, Investigation, Writing – original draft. **Ramar Rajamanikandan:** Methodology, Validation, Investigation, Visualization. **Heongkyu Ju:** Conceptualization, Validation, Investigation, Resources, Writing – review & editing, Visualization, Supervision, Funding acquisition.

Acknowledgments: This work was supported by the Gachon University research fund of 2023 (GCU-202300980001) and also supported by the National Research Foundation of Korea (NRF) grants funded by the Korean government (MSIT) (No. RS-2023-00279149).

Conflicts of interest: There are no conflicts to declare.

References

1. Lone, I.A., Rohit, J.V., 2025. Carbon dots encapsulated metal-organic frameworks: An emerging optical sensors for monitoring of environmental pollutants. *Inorganic Chemistry Communications*, 114918.
2. Xia, C., Zhu, S., Feng, T., Yang, M., Yang, B., 2019. Evolution and synthesis of carbon dots: from carbon dots to carbonized polymer dots. *Advanced Science*, 6(23), 1901316.
3. Falara, P.P., Zourou, A., Kordatos, K.V., 2022. Recent advances in Carbon Dots/2-D hybrid materials. *Carbon*, 195, 219-245.
4. Mkhari, O., Ntuli, T.D., Coville, N.J., Nxumalo, E.N., Maubane-Nkadimeng, M.S., 2023. Supported carbon-dots: A review. *Journal of Luminescence*, 255, 119552.
5. Chen, B.B., Liu, M.L., Li, C.M., Huang, C.Z., 2019. Fluorescent carbon dots functionalization. *Advances in colloid and interface science*, 270, 165-190.
6. Parani, S., Choi, E.Y., Oluwafemi, O.S., Song, J.K., 2023. Carbon dot engineered membranes for separation—a comprehensive review and current challenges. *Journal of Materials Chemistry A*, 11(44), 23683-23719.
7. Liu, C., Lin, X., Liao, J., Yang, M., Jiang, M., Huang, Y., Du, Z., Chen, L., Fan, S., Huang, Q., 2024. Carbon dots-based dopamine sensors: recent advances and challenges. *Chinese Chemical Letters*, 35(12), 109598.
8. Zuo, P., Lu, X., Sun, Z., Guo, Y., He, H., 2016. A review on syntheses, properties, characterization and bioanalytical applications of fluorescent carbon dots. *Microchimica Acta*, 183(2), 519-542.
9. Lim, S.Y., Shen, W., Gao, Z., 2015. Carbon quantum dots and their applications. *Chemical Society Reviews*, 44(1), 362-381.
10. Sasikumar, K., Rajamanikandan, R., Ju, H., 2023. Nitrogen-and sulfur-codoped strong green fluorescent carbon dots for the highly specific quantification of quercetin in food samples. *Materials*, 16(24), 7686.

11. Kamal, A., Hong, S., Ju, H., 2025. Carbon quantum dots: synthesis, characteristics, and quenching as biocompatible fluorescent probes. *Biosensors*, 15(2), 99.
12. Wang, B., Wang, H., Hu, Y., Waterhouse, G.I., Lu, S., 2023. Carbon dot based multicolor electroluminescent LEDs with nearly 100% exciton utilization efficiency. *Nano Letters*, 23(18), 8794-8800.
13. Rajamanikandan, R., Prabakaran, D.S., Sasikumar, K., Seok, J.S., Lee, G., Ju, H., 2024. Biocompatible bright orange emissive carbon dots: Multifunctional nanoprobe for highly specific sensing toxic Cr(VI) ions and mitochondrial targeting cancer cell imaging. *Talanta Open*, 10, 100353.
14. Dhenadhayalan, N., Lin, K.C., Saleh, T.A., 2020. Recent advances in functionalized carbon dots toward the design of efficient materials for sensing and catalysis applications. *Small*, 16(1), 1905767.
15. Bartkowski, M., Zhou, Y., Nabil Amin Mustafa, M., Eustace, A.J., Giordani, S., 2024. CARBON DOTS: bioimaging and anticancer drug delivery. *Chemistry—A European Journal*, 30(19), e202303982.
16. Sasikumar, K., Rajamanikandan, R., Ju, H., 2025. Bright green fluorescent carbon dots: Smartphone-assisted sensing platform for arsenic detection in water and mitochondrial-targeted imaging. *Microchemical Journal*, 115309.
17. Dong, W., Wang, R., Gong, X., Dong, C., 2019. An efficient turn-on fluorescence biosensor for the detection of glutathione based on FRET between N, S dual-doped carbon dots and gold nanoparticles. *Analytical and Bioanalytical Chemistry*, 411(25), 6687-6695.
18. Wang, X., Liu, Y., Wang, Q., Bu, T., Sun, X., Jia, P., Wang, L., 2021. Nitrogen, silicon co-doped carbon dots as the fluorescence nanoprobe for trace p-nitrophenol detection based on inner filter effect. *Spectrochimica Acta Part A: Molecular and Biomolecular Spectroscopy*, 244, 118876.
19. Wang, Q., Zhang, H., Yu, D., Qin, W., Wu, X., 2022. Ultra-sensitive and stable N-doped carbon dots for selective detection of uranium through electron transfer induced $\text{UO}_2^{+}(\text{V})$ sensing mechanism. *Carbon*, 198, 162-170.
20. Tang, X., Yu, H., Bui, B., Wang, L., Xing, C., Wang, S., Chen, M., Hu, Z., Chen, W., 2021. Nitrogen-doped fluorescence carbon dots as multi-mechanism detection for iodide and curcumin in biological and food samples. *Bioactive materials*, 6(6), 1541-1554.
21. Sharifi, M., Pourasl, M.H., Tajalli, H., Khalilzadeh, B., Isildak, I., 2025. Advances in biosensors for wastewater quality assessment. *TrAC Trends in Analytical Chemistry*, 195, 118622.
22. Pawar, S., Kaja, S., Nag, A., 2020. Red-emitting carbon dots as a dual sensor for In^{3+} and Pd^{2+} in water. *ACS omega*, 5(14), 8362-8372.
23. Liu, B., Zhuang, J., Wei, G., 2020. Recent advances in the design of colorimetric sensors for environmental monitoring. *Environmental Science: Nano*, 7(8), 2195-2213.
24. Mandal, P., Sahoo, D., Sarkar, P., Chakraborty, K., Das, S., 2019. Fluorescence turn-on and turn-off sensing of pesticides by carbon dot-based sensor. *New Journal of Chemistry*, 43(30), 12137-12151.
25. Durgapameshwari, M., Kaviya, K., Prabakaran, D.S., Santhamoorthy, M., Rajamanikandan, R., Al-Ansari, M.M., Mani, K.S., 2024. Designing a Simple Quinoline-Based Chromo-Fluorogenic Receptor for Highly Specific Quantification of Copper (II) Ions: Environmental and Bioimaging Applications. *Luminescence*, 39(12), e70068.
26. Sadeque, M.S.B., Chowdhury, H.K., Rafique, M., Durmuş, M.A., Ahmed, M.K., Hasan, M.M., Erbaş, A., Sarpkaya, İ., Inci, F., Ordu, M., 2023. Hydrogel-integrated optical fiber sensors and their applications: a comprehensive review. *Journal of Materials Chemistry C*, 11(28), 9383-9424.
27. Tran, N.H.T., Kim, J., Phan, T.B., Khym, S., Ju, H., 2017. Label-free optical biochemical sensors via liquid-cladding-induced modulation of waveguide modes. *ACS Applied Materials & Interfaces*, 9(37), 31478-31487.
28. Tran, V.T., Yoon, W.J., Lee, J.H., Ju, H., 2018. DNA sequence-induced modulation of bimetallic surface plasmons in optical fibers for sub-ppq (parts-per-quadrillion) detection of mercury ions in water. *Journal of Materials Chemistry A*, 6(46), 23894-23902.
29. Fu, R., Chen, X., Yan, X., Li, H., Hu, T., Wei, L., Qu, Y., Cheng, T., 2024. Optical fiber sensors for heavy metal ion sensing. *Journal of materials science & technology*, 189, 110-131.
30. Tran, N.H.T., Phan, T.B., Nguyen, T.T., Ju, H., 2021. Coupling of silver nanoparticle-conjugated fluorescent dyes into optical fiber modes for enhanced signal-to-noise ratio. *Biosensors and Bioelectronics*, 176, 112900.

31. Elsherif, M., Salih, A.E., Muñoz, M.G., Alam, F., AlQattan, B., Antonysamy, D.S., Zaki, M.F., Yetisen, A.K., Park, S., Wilkinson, T.D., Butt, H., 2022. Optical fiber sensors: Working principle, applications, and limitations. *Advanced Photonics Research*, 3(11), 2100371.
32. Wen, H.Y., Hsu, H.C., Tsai, Y.T., Feng, W.K., Lin, C.L., Chiang, C.C., 2021. U-shaped optical fiber probes coated with electrically doped GQDs for humidity measurements. *Polymers*, 13(16), 2696.
33. Gonçalves, H.M., Duarte, A.J., da Silva, J.C.E., 2010. Optical fiber sensor for Hg(II) based on carbon dots. *Biosensors and Bioelectronics*, 26(4), 1302-1306.
34. Wang, N., Tian, W., Zhang, H., Yu, X., Yin, X., Du, Y., Li, D., 2021. An easily fabricated high performance Fabry-Perot optical fiber humidity sensor filled with graphene quantum dots. *Sensors*, 21(3), 806.
35. Vyas, T., Jaiswal, S., Choudhary, S., Kodgire, P., Joshi, A., 2024. Recombinant Organophosphorus acid anhydrolase (OPAA) enzyme-carbon quantum dot (CQDs)-immobilized thin film biosensors for the specific detection of Ethyl Paraoxon and Methyl Parathion in water resources. *Environmental research*, 243, 117855.
36. Nazri, N.A.A., Azeman, N.H., Bakar, M.H.A., Mobarak, N.N., Masran, A.S., Zain, A.R.M., Mahdi, M.A., Saputro, A.G., Wung, T.D.K., Luo, Y., Bakar, A.A.A., 2024. Polymeric carbon quantum dots as efficient chlorophyll sensor-analysis based on experimental and computational investigation. *Optics & Laser Technology*, 170, 110259.
37. Li, M., Singh, R., Wang, Y., Marques, C., Zhang, B., Kumar, S., 2022. Advances in novel nanomaterial-based optical fiber biosensors—A review. *Biosensors*, 12(10), 843.
38. Nazri, N.A.A., Azeman, N.H., Luo, Y., Bakar, A.A.A., 2021. Carbon quantum dots for optical sensor applications: A review. *Optics & Laser Technology*, 139, 106928.
39. Sasikumar, K., Rajamanikandan, R., Ju, H., 2024. Inner filter effect-based highly sensitive quantification of 4-nitrophenol by strong fluorescent N, S co-doped carbon dots. *Carbon Letters*, 34(2), 851-863.
40. Sasikumar, K., Prabakaran, D.S., Rajamanikandan, R., Ju, H., 2024. Yellow Emissive Carbon Dots—A Robust Nanoprobe for Highly Sensitive Quantification of Jaundice Biomarker and Mitochondria Targeting in Cancer Cells. *ACS Applied Bio Materials*, 7(10), 6730-6739.
41. Zhang, H., Guo, X., Jian, K., Fu, L., Zhao, X., 2023. Rapid preparation of long-wavelength emissive carbon dots for information encryption using the microwave-assisted method. *Inorganic Chemistry*, 62(34), 13847-13856.
42. Dager, A., Uchida, T., Maekawa, T., Tachibana, M., 2019. Synthesis and characterization of mono-disperse carbon quantum dots from fennel seeds: photoluminescence analysis using machine learning. *Scientific reports*, 9(1), 14004.
43. Onyancha, R.B., Ukhurebor, K.E., Aigbe, U.O., Osibote, O.A., Kusuma, H.S., Darmokoeseoemo, H., 2022. A methodical review on carbon-based nanomaterials in energy-related applications. *Adsorption Science & Technology*, 2022, 4438286.
44. Calabro, R.L., Yang, D.S., Kim, D.Y., 2019. Controlled nitrogen doping of graphene quantum dots through laser ablation in aqueous solutions for photoluminescence and electrocatalytic applications. *ACS Applied Nano Materials*, 2(11), 6948-6959.
45. González-González, R.B., González, L.T., Madou, M., Leyva-Porras, C., Martínez-Chapa, S.O., Mendoza, A., 2022. Synthesis, purification, and characterization of carbon dots from non-activated and activated pyrolytic carbon black. *Nanomaterials*, 12(3), 298.
46. Magesh, V., Sundramoorthy, A.K., Ganapathy, D., 2022. Recent advances on synthesis and potential applications of carbon quantum dots. *Frontiers in materials*, 9, 906838.
47. Wang, Z., Changotra, R., Dasog, M., Selopal, G.S., Yang, J., He, Q.S., 2025. Carbon quantum dots: Synthesis via hydrothermal processing, doping strategies, integration with photocatalysts, and their application in photocatalytic hydrogen production. *Sustainable Materials and Technologies*, 44, e01386.
48. Cai, Y., Wang, M., Liu, M., Zhang, J., Zhao, Y., 2022. A Portable Optical Fiber Sensing Platform Based on Fluorescent Carbon Dots for Real-Time pH Detection. *Advanced Materials Interfaces*, 9(4), 2101633.
49. Shen, J., Zheng, X., Lin, L., Xu, H., Xu, G., 2023. Reaction time-controlled synthesis of multicolor carbon dots for white light-emitting diodes. *ACS Applied Nano Materials*, 6(4), 2478-2490.

50. Liu, J., Li, D., Zhang, K., Yang, M., Sun, H., Yang, B., 2018. One-step hydrothermal synthesis of nitrogen-doped conjugated carbonized polymer dots with 31% efficient red emission for in vivo imaging. *Small*, 14(15), 1703919.
51. Yat, Y.D., Foo, H.C.Y., Tan, I.S., Lam, M.K., Lim, S., 2022. Carbon dots and miniaturizing fabrication of portable carbon dot-based devices for bioimaging, biosensing, heavy metal detection and drug delivery applications. *Journal of Materials Chemistry C*, 10(41), 15277-15300.
52. Liu, C., Ye, F., Fu, Y., 2026. Nanoscale light warriors: a review of carbon dot-based optical sensors for insecticide residue detection in food and ecosystems. *Talanta*, 296, 128445.
53. Inoue, K., Suzuki, R., Kaneda, Y., Tanimura, M., Shinozaki, K., Tachibana, M., 2025. Effects of pyrolysis temperature on plant-seed-derived carbon dots. *Journal of Materials Chemistry C*, 13(45), 22832-22840.
54. Etefa, H.F., Tessema, A.A., Dejene, F.B., 2024. Carbon dots for future prospects: synthesis, characterizations and recent applications: a review (2019–2023). *C*, 10(3), 60.
55. Lamba, R., Yukta, Y., Mondal, J., Kumar, R., Pani, B., Singh, B., 2024. Carbon dots: Synthesis, characterizations, and recent advancements in biomedical, optoelectronics, sensing, and catalysis applications. *ACS Applied Bio Materials*, 7(4), 2086-2127.
56. Gonçalves, H.M., Duarte, A.J., Davis, F., Higson, S.P., da Silva, J.C.E., 2012. Layer-by-layer immobilization of carbon dots fluorescent nanomaterials on single optical fiber. *Analytica chimica acta*, 735, 90-95.
57. Ajith, M.P., Pardhiya, S., Rajamani, P., 2022. Carbon dots: an excellent fluorescent probe for contaminant sensing and remediation. *Small*, 18(15), 2105579.
58. Kang, S., Jeong, Y.K., Ryu, J.H., Son, Y., Kim, W.R., Lee, B., Jung, K.H., Kim, K.M., 2020. Pulsed laser ablation based synthetic route for nitrogen-doped graphene quantum dots using graphite flakes. *Applied Surface Science*, 506, 144998.
59. Ge, G., Li, L., Wang, D., Chen, M., Zeng, Z., Xiong, W., Wu, X., Guo, C., 2021. Carbon dots: synthesis, properties and biomedical applications. *Journal of Materials Chemistry B*, 9(33), 6553-6575.
60. Gao, W., He, J., Chen, L., Meng, X., Ma, Y., Cheng, L., Tu, K., Gao, X., Liu, C., Zhang, M., Fan, K., 2023. Deciphering the catalytic mechanism of superoxide dismutase activity of carbon dot nanozyme. *Nature communications*, 14(1), 160.
61. Peng, H., Travas-Sejdic, J., 2009. Simple aqueous solution route to luminescent carbogenic dots from carbohydrates. *Chemistry of Materials*, 21(23), 5563-5565.
62. Shinde, D.B., Pillai, V.K., 2012. Electrochemical preparation of luminescent graphene quantum dots from multiwalled carbon nanotubes. *Chemistry–A European Journal*, 18(39), 12522-12528.
63. Ming, H., Ma, Z., Liu, Y., Pan, K., Yu, H., Wang, F., Kang, Z., 2012. Large scale electrochemical synthesis of high quality carbon nanodots and their photocatalytic property. *Dalton transactions*, 41(31), 9526-9531.
64. Chowdhury, S., Rooj, B., Dutta, A., Mandal, U., 2018. Review on recent advances in metal ions sensing using different fluorescent probes. *Journal of fluorescence*, 28(4), 999-1021.
65. Ali, Z., Ullah, R., Tuzen, M., Ullah, S., Rahim, A., Saleh, T.A., 2023. Colorimetric sensing of heavy metals on metal doped metal oxide nanocomposites: A review. *Trends in Environmental Analytical Chemistry*, 37, e00187.
66. Panda, S.K., Mishra, S., Singh, A.K., 2021. Recent progress in the development of MOF-based optical sensors for Fe³⁺. *Dalton Transactions*, 50(21), 7139-7155.
67. Lin, H., Huang, J., Ding, L., 2019. A recyclable optical fiber sensor based on fluorescent carbon dots for the determination of ferric ion concentrations. *Journal of lightwave technology*, 37(18), 4815-4822.
68. Bian, Z., Xu, Q., Chu, F., Hou, S., Xue, L., Hu, A., Dai, C., Feng, Y., Zhou, B., 2024. Fe³⁺ Sensing Based on Hydrogel Optical Fiber Doped with Nitrogen Carbon Dots. *Journal of Electronic Materials*, 53(2), 642-651.
69. Cai, Y., Zhang, J., Zhang, M., Wang, M., Zhao, Y., 2022. The optical fiber sensing platform for ferric ions detection: A practical application for carbon quantum dots. *Sensors and Actuators B: Chemical*, 364, 131857.
70. Cai, Y., Zhang, J., Jiang, T., Wang, J., Zhao, Y., 2023. Ratiometric fluorescence optical fiber sensing for on-site ferric ions detection using single-emission carbon quantum dots. *IEEE Transactions on Instrumentation and Measurement*, 72, 1-8.
71. Adkisson, A., Gouramanis, D., Kim, K.J., Burgess, W., Siefert, N., Crawford, S., 2025. A Synthetic Pathway for Producing Carbon Dots for Detecting Iron Ions Using a Fiber Optic Spectrometer. *Sensors*, 25(19), 6066.

72. Fu, R., Yan, X., Hu, T., Li, H., Cheng, T., 2025. Carbon Dots-Based Surface Plasmon Resonance Manganese Ion Fiber Sensor for Multi-Use Scenarios. *Photonic Sensors*, 15(3), 250311.
73. Zhou, Y., Huang, X., Xia, B., Chen, X., Jing, X., Wang, N., Li, J., 2025. An ultrasensitive optical fiber SPR sensor enhanced by functionalized carbon quantum dots for Fe³⁺ measurement. *Journal of Alloys and Compounds*, 1030, 180784.
74. Yap, S.H.K., Chan, K.K., Zhang, G., Tjin, S.C., Yong, K.T., 2019. Carbon dot-functionalized interferometric optical fiber sensor for detection of ferric ions in biological samples. *ACS applied materials & interfaces*, 11(31), 28546-28553.
75. Mehta, P.K., Lee, J., Oh, E.T., Park, H.J., Lee, K.H., 2023. Ratiometric fluorescence sensing system for lead ions based on self-assembly of bioprobes triggered by specific Pb²⁺-peptide interactions. *ACS applied materials & interfaces*, 15(11), 14131-14145.
76. Vyas, T., Kumar, H., Choudhary, S., Joshi, A., 2024. Carbon quantum dot (CQD)-dithizone-based thin-film chemical sensors for the specific detection of lead ions in water resources. *Environmental Science: Water Research & Technology*, 10(11), 2858-2868.
77. Tran, V.T., Tran, N.H.T., Nguyen, T.T., Yoon, W.J., Ju, H., 2018. Liquid cladding mediated optical fiber sensors for copper ion detection. *Micromachines*, 9(9), 471.
78. Vyas, T., Choudhary, S., Sharan Rathnam, S., Joshi, A., 2023. Fiber-Optic Detection of Aluminum and Copper in Real Water Samples Using Enzyme-Carbon Quantum Dot (CQD)-Based Thin-Film Biosensors. *ACS ES&T Engineering*, 4(3), 694-705.
79. Vyas, T., Joshi, A., 2024. Chemical sensor thin film-based carbon quantum dots (CQDs) for the detection of heavy metal count in various water matrices. *Analyst*, 149(4), 1297-1309.
80. Crawford, S.E., Kim, K.J., Baltrus, J.P., 2022. A portable fiber optic sensor for the luminescent sensing of cobalt ions using carbon dots. *Journal of Materials Chemistry C*, 10(43), 16506-16516.
81. Sapna, K., Sonia, J., Shim, Y.B., Arun, A.B., Prasad, K.S., 2022. Au nanoparticle-based disposable electrochemical sensor for detection of leptospirosis in clinical samples. *ACS Applied Nano Materials*, 5(9), 12454-12463.
82. Zainuddin, N.H., Chee, H.Y., Rashid, S.A., Ahmad, M.Z., Bakar, M.H.A., Mahdi, M.A., Yaacob, M.H., 2023. Carbon quantum dots functionalized tapered optical fiber for highly sensitive and specific detection of Leptospira DNA. *Optics & Laser Technology*, 157, 108696.
83. Zainuddin, N.H., Chee, H.Y., Rashid, S.A., Ahmad, M.Z., Zan, Z., Bakar, M.H.A., Alresheedi, M.T., Mahdi, M.A., Yaacob, M.H., 2023. Enhanced detection sensitivity of Leptospira DNA using a post-deposition annealed carbon quantum dots integrated tapered optical fiber biosensor. *Optical Materials*, 141, 113926.
84. Zhang, Y., Ding, L., Zhang, H., Wang, P., Li, H., 2022. A new optical fiber biosensor for acetylcholine detection based on pH sensitive fluorescent carbon quantum dots. *Sensors and Actuators B: Chemical*, 369, 132268.
85. Sangubotla, R., Kim, J., 2021. Fiber-optic biosensor based on the laccase immobilization on silica-functionalized fluorescent carbon dots for the detection of dopamine and multi-color imaging applications in neuroblastoma cells. *Materials Science and Engineering: C*, 122, 111916.
86. Xiong, H., Ding, L., Xu, B., Liang, B., Yuan, F., 2021. A versatile optical fiber sensor comprising an excitation-independent carbon quantum dots/cellulose acetate composite film for adrenaline detection. *IEEE Sensors Journal*, 21(9), 10392-10399.
87. Yi, Z., Xiao, S., Kang, X., Long, F., Zhu, A., 2024. Bifunctional MOF-encapsulated cobalt-doped carbon dots nanozyme-powered chemiluminescence/fluorescence dual-mode detection of aflatoxin B1. *ACS Applied Materials & Interfaces*, 16(13), 16494-16504.
88. Kim, J., Son, C., Choi, S., Yoon, W.J., Ju, H., 2018. A plasmonic fiber based glucometer and its temperature dependence. *Micromachines*, 9(10), 506.
89. Van Tam, T., Hur, S.H., Chung, J.S., Choi, W.M., 2021. Novel paper-and fiber optic-based fluorescent sensor for glucose detection using aniline-functionalized graphene quantum dots. *Sensors and Actuators B: Chemical*, 329, 129250.

90. Yu, S., Ding, L., Lin, H., Wu, W., Huang, J., 2019. A novel optical fiber glucose biosensor based on carbon quantum dots-glucose oxidase/cellulose acetate complex sensitive film. *Biosensors and Bioelectronics*, 146, 111760.
91. Vyas, T., Kumar, H., Nagpure, G., Joshi, A., 2024. Fiber-optic thin film chemical sensor of 2, 4 dinitro-1-chlorobenzene and carbon quantum dots for the point-of-care detection of hydrazine in water samples. *Environmental Science: Water Research & Technology*, 10(6), 1481-1491.
92. Wu, W., Huang, J., Ding, L., Lin, H., Yu, S., Yuan, F., Liang, B., 2021. A real-time and highly sensitive fiber optic biosensor based on the carbon quantum dots for nitric oxide detection. *Journal of Photochemistry and Photobiology A: Chemistry*, 405, 112963.
93. Vyas, T., Gogoi, M., Joshi, A., 2023. Fluorescent fiber-optic device sensor based on carbon quantum dot (CQD) thin films for dye detection in water resources. *Analyst*, 148(20), 5178-5189.

Disclaimer/Publisher's Note: The statements, opinions and data contained in all publications are solely those of the individual author(s) and contributor(s) and not of MDPI and/or the editor(s). MDPI and/or the editor(s) disclaim responsibility for any injury to people or property resulting from any ideas, methods, instructions or products referred to in the content.